New Phytologist

Research

Asymmetric genome merging leads to gene expression novelty through nucleo-cytoplasmic disruptions and transcriptomic shock in *Chlamydomonas* triploids

Lucas Prost-Boxoen[1,2,3], Quinten Bafort[1,2,3], Antoine Van de Vloet[1,2,3], Fabricio Almeida-Silva[1,2], Yunn Thet Paing[1,2], Griet Casteleyn[1,2,3], Sofie D'hondt[3], Olivier De Clerck[3] and Yves Van de Peer[1,2,3,4,5]

[1]Department of Plant Biotechnology and Bioinformatics, Ghent University, Ghent, 9052, Belgium; [2]VIB Center for Plant Systems Biology, VIB, Ghent, 9052, Belgium; [3]Department of Biology, Ghent University, Ghent, 9052, Belgium; [4]Department of Biochemistry, Genetics and Microbiology, Centre for Microbial Ecology and Genomics, University of Pretoria, Pretoria, 0028, South Africa; [5]College of Horticulture, Academy for Advanced Interdisciplinary Studies, Nanjing Agricultural University, Nanjing, 210095, China

Authors for correspondence:
Yves Van de Peer
Email: yves.vandepeer@psb.vib-ugent.be

Lucas Prost-Boxoen
Email: lucas.prost@psb.vib-ugent.be

Received: *8 August 2024*
Accepted: *21 October 2024*

New Phytologist (2025) **245:** 869–884
doi: 10.1111/nph.20249

Key words: allopolyploidy, *Chlamydomonas reinhardtii*, experimental evolution laboratory natural selection (LNS), genome merging, RNA-Seq, transcriptomics.

Summary

- Genome merging is a common phenomenon causing a wide range of consequences on phenotype, adaptation, and gene expression, yet its broader implications are not well-understood. Two consequences of genome merging on gene expression remain particularly poorly understood: dosage effects and evolution of expression.
- We employed *Chlamydomonas reinhardtii* as a model to investigate the effects of asymmetric genome merging by crossing a diploid with a haploid strain to create a novel triploid line. Five independent clonal lineages derived from this triploid line were evolved for 425 asexual generations in a laboratory natural selection experiment.
- Utilizing fitness assays, flow cytometry, and RNA-Seq, we assessed the immediate consequences of genome merging and subsequent evolution. Our findings reveal substantial alterations in genome size, gene expression, protein homeostasis, and cytonuclear stoichiometry. Gene expression exhibited expression-level dominance and transgressivity (i.e. expression level higher or lower than either parent). Ongoing expression-level dominance and a pattern of 'functional dominance' from the haploid parent was observed.
- Despite major genomic and nucleo-cytoplasmic disruptions, enhanced fitness was detected in the triploid strain. By comparing gene expression across generations, our results indicate that proteostasis restoration is a critical component of rapid adaptation following genome merging in *Chlamydomonas reinhardtii* and possibly other systems.

Introduction

Polyploidy, which occurs when cells or organisms possess more than two complete sets of genomes, comes in two types: autopolyploidy, arising from whole genome duplication (WGD), and allopolyploidy, resulting from WGD combined with genome merging, i.e. hybridization (Stebbins, 1947). It is, however, often more accurate to describe allo- and autopolyploids as extremes of a continuum along the genetic distance between parental genotypes (Soltis *et al.*, 2010). This 'mutation' significantly impacts all biological levels and is prevalent across eukaryotes, but particularly affecting the evolution of angiosperms (Otto & Whitton, 2000; Albertin & Marullo, 2012; Fox *et al.*, 2020). Indeed, polyploidy is prevalent in contemporary plants, particularly in crops and invasive species, and it seems to confer robustness during environmental stress and upheavals (Fawcett *et al.*, 2009; Soltis *et al.*, 2009; Tate *et al.*, 2009; te Beest *et al.*, 2012; Vanneste *et al.*, 2014; Van de Peer *et al.*, 2017; Shimizu, 2022).

Genome doubling and merging have substantial influences across all levels of cellular biology (Comai, 2005; Doyle & Coate, 2019; Bomblies, 2020). A frequently observed consequence of polyploidy is cell size increase (Otto, 2007; Kwak *et al.*, 2017; Doyle & Coate, 2019; Bomblies, 2020), although this relationship exhibits complex dynamics, i.e. that ploidy-dependent increase of cell size follows neither a linear nor a constant pattern (Tsukaya, 2013). Cell size increase resulting from polyploidization can subsequently affect transcriptome size and transcription (Wu *et al.*, 2010; Marguerat & Bähler, 2012; Doyle & Coate, 2019). Additionally, genome doubling and, in particular, genome merging have been identified to induce a 'genome shock' (McClintock, 1984), initiating fast and significant alterations to the genome (Otto, 2007). WGD is also expected to alter the balance between the different genomes of plant cells, i.e.

the stoichiometry between nucleus, plastids, and mitochondria, known as cytonuclear stoichiometry (Doyle & Coate, 2019; Song *et al.*, 2020). Sharbrough *et al.* (2017) proposed four mechanisms for maintaining cytonuclear stoichiometry in polyploid plants: larger organelles, increased organellar genome copy numbers, larger cells with more organelles, and recovery of cytonuclear gene expression balance through increased cytoplasmic or reduced nuclear gene expression per genome copy. Evidence shows that nascent polyploid plants can compensate for the increased nuclear genome dosage through higher cytosolic genome copy numbers (Coate *et al.*, 2020; Fernandes Gyorfy *et al.*, 2021) or by scaling gene expression to maintain cytonuclear expression ratios after WGD (Forsythe *et al.*, 2022), although this is not always observed (Oberprieler *et al.*, 2019).

Genome merging likely has a more profound impact on transcription than genome duplication (Doyle *et al.*, 2008; Chelaifa *et al.*, 2010; Parisod *et al.*, 2010; Spoelhof *et al.*, 2017; Behling *et al.*, 2022). In allopolyploids, gene expression frequently deviates from the additivity hypothesis, which assumes that the gene expression levels are the average of those in the parent species, revealing complex parental legacies (Adams *et al.*, 2003; Osborn *et al.*, 2003; Otto, 2003; Adams & Wendel, 2005; Auger *et al.*, 2005; Chelaifa *et al.*, 2010; Yoo *et al.*, 2013, 2014). A commonly observed pattern is expression-level dominance (ELD), or genome dominance, in which the expression of a given gene is similar to only one of the parents (Rapp *et al.*, 2009; Flagel & Wendel, 2010; Grover *et al.*, 2012; Yoo *et al.*, 2013; Combes *et al.*, 2015; Edger *et al.*, 2017; Bird *et al.*, 2018; Li *et al.*, 2018; Wu *et al.*, 2018; Nieto Feliner *et al.*, 2020; Wei *et al.*, 2021). Allopolyploids can also exhibit transgressive expression, where the gene expression is either greater or lesser than that of both progenitors (Rapp *et al.*, 2009; Flagel & Wendel, 2010; Yoo *et al.*, 2013). Nonetheless, some allopolyploids exhibit additive expression (Chagué *et al.*, 2010; Chelaifa *et al.*, 2013). Moreover, ELD seems influenced by environmental factors (Bardil *et al.*, 2011; Shimizu-Inatsugi *et al.*, 2017), tissue specificity (Li *et al.*, 2014, 2020), and developmental stage (Jia *et al.*, 2022). Gene expression novelty created upon genome merging has been referred to as a 'transcriptomic shock' (Buggs *et al.*, 2011). Such alterations might drive the development of novel phenotypes that could be key to the adaptive success of allopolyploids (Hegarty & Hiscock, 2009).

Two poorly understood consequences of genome merging on gene expression are genome dosage effects and the evolution of expression. Asymmetric genome inheritance, via gene dosage (the number of copies of a gene), could cause asymmetric parental legacies in gene expression in the allopolyploid, *for example* in wheat (Qi *et al.*, 2012) and the fish *Cobitis* (Bartoš *et al.*, 2019). It is crucial to track newly formed allopolyploids immediately postmerging to understand the dynamics of gene expression in the first generations after genome merging. Employing transgenerational comparative transcriptomics can elucidate the trends in gene expression following allopolyploidization. Research on wheat presents varied findings regarding postpolyploidization gene expression, as shown in the studies of Chagué *et al.* (2010) and Qi *et al.* (2012). Both studies confirm the immediate alterations in gene expression patterns upon genome merging. However, while Chagué *et al.* (2010) reported stability within specific gene expression patterns, Qi *et al.* (2012) observed predominantly stochastic variations. This divergence highlights the need for further investigation to understand the mechanisms behind gene expression patterns in allopolyploids and their evolutionary impacts.

Chlamydomonas reinhardtii Dangeard is a single-celled green alga belonging to the Chlorophyta phylum. This model species is easy to cultivate and manage in the laboratory and has a short generation time. Given these attributes, *C. reinhardtii* serves as a model organism for fundamental research on genetics, photosynthesis, and structural biology (Harris, 2001; Sasso *et al.*, 2018; Salomé & Merchant, 2019). This microalga species is also valuable in applied research domains, including biopharmaceuticals and biofuel production (Scranton *et al.*, 2015; Kwak *et al.*, 2017). Additionally, its rapid doubling time of 8 h, ease of cultivation, and minimal space requirements make *C. reinhardtii* particularly effective for studying evolution (Bell, 1997; Harris, 2001; Ratcliff *et al.*, 2013; Bafort *et al.*, 2023).

Here, we employ *C. reinhardtii* to examine the effects of asymmetric genome merging on fitness, expression patterns, and evolutionary changes in genome size and gene expression over 425 generations of a laboratory natural selection (LNS) experiment. To our knowledge, this is the first study to examine the effects of polyploidy over several hundred generations in green plants in a controlled laboratory environment. By crossing a haploid and a diploid strain to create triploid lines, we analyzed the impact using fitness assessment, flow cytometry, and RNA sequencing at three time points: the ancestor (G0), generation 225, and generation 425. Our results reveal significant changes in gene expression, with no clear genome dominance, and suggest 'functional dominance' from the haploid parent. The study highlights disruptions in cytonuclear balance, potential disturbances in proteostasis, and a rapid and uniform reduction in genome size in all experimental lines, reflecting the complex cellular responses to genome merging. Despite the major nucleo-cytoplasmic changes, the newly formed triploid strain revealed increased fitness compared with its parental strains.

Materials and Methods

Strains and experimental conditions

Chlamydomonas reinhardtii strains CC-1067 (*arg2*, *mt*+, haploid) and CC-1820 (*arg 7-2*, *mt*−, diploid, mislisted as haploid by the Chlamydomonas Resource Center at the time of acquisition) were obtained from the Chlamydomonas Resource Center. A triploid strain was formed by fusion of CC-1067 and CC-1820 and complementation of the auxotrophic *arg* mutations, following the method of Ebersold (1967). When not in active cultivation, the strains were preserved on Tris-acetate-phosphate (TAP) agar plates containing arginine under low-light conditions (*c.* 50 μmol m^{-2} s^{-1} PPFD) at 22°C.

The triploid strain was bottlenecked to a single cell, followed by its rapid division into five separate, independent lines,

Table 1 Overview of the *Chlamydomonas reinhardtii* strains used in this study.

Line	Label	CRC	Ploidy	Generation	Description	Techniques
Diploid parent	2N parent	CC-1820	2 N	NA	mt- parent, arginine synthesis deficient (arg7-2)	RNA-Seq, Fitness assay, Flow cytometry
Haploid parent	1N parent	CC-1067	1 N	NA	mt + parent, arginine synthesis deficient (arg2)	RNA-Seq, Fitness assay, Flow cytometry
Triploid progeny	3N G0	NA	3 N	0	Lab-derived progeny from CC-1820/CC-1067 cross, arginine-deficiency complemented	RNA-Seq, Fitness assay, Flow cytometry
Line 1 G225	3N G225	NA	*c.* 3N	225	Line derived from triploid progeny, observed at G225	RNA-Seq, Fitness assay, Flow cytometry
Line 2 G225	3N G225	NA	*c.* 3N	225	Line derived from triploid progeny, observed at G225	RNA-Seq, Fitness assay, Flow cytometry
Line 3 G225	3N G225	NA	*c.* 3N	225	Line derived from triploid progeny, observed at G225	RNA-Seq, Fitness assay, Flow cytometry
Line 4 G225	3N G225	NA	*c.* 3N	225	Line derived from triploid progeny, observed at G225	RNA-Seq, Fitness assay, Flow cytometry
Line 5 G225	3N G225	NA	*c.* 3N	225	Line derived from triploid progeny, observed at G225	RNA-Seq, Fitness assay, Flow cytometry
Line 1 G425	3N G425	NA	*c.* 3N	425	Line derived from triploid progeny, observed at G425	RNA-Seq, Fitness assay, Flow cytometry
Line 2 G425	3N G425	NA	*c.* 3N	425	Line derived from triploid progeny, observed at G425	RNA-Seq, Fitness assay, Flow cytometry
Line 3 G425	3N G425	NA	*c.* 3N	425	Line derived from triploid progeny, observed at G425	RNA-Seq, Fitness assay, Flow cytometry
Line 4 G425	3N G425	NA	*c.* 3N	425	Line derived from triploid progeny, observed at G425	RNA-Seq, Fitness assay, Flow cytometry
Line 5 G425	3N G425	NA	*c.* 3N	425	Line derived from triploid progeny, observed at G425	RNA-Seq, Fitness assay, Flow cytometry

CRC refers to the Chlamydomonas Resource Center. Strains marked as 'NA' in the CRC column were generated in our laboratory and have not been assigned a CRC label.

initiating the LNS experiment. The experimental lines were cultivated in 5 ml arginine-supplemented TAP medium within Erlenmeyer flasks at 23°C, under a light intensity of 150 µmol m^{-2} s^{-1} PPFD and agitated at a rate of 150 rpm. Routine transfers of the lines were performed, consisting of transferring 5% of the volume into fresh medium, occurring once or twice per week.

Evolving lines were cryopreserved at regular time intervals to allow future comparative analyses with evolving lines. After 99 transfers, we thawed the ancestral strains (CC-1067, CC-1820, and the triploid line following bottlenecking and before line division, thereafter named 1N parent, 2N parent, and 3N G0, respectively) and the experimental triploid lines from the 52nd transfer (3N G225).

The number of generations was calculated using the formula:

$$N_g = N_t \times \log_2(D)$$

where N_g represents the number of mitotic generations, N_t denotes the number of transfers, and D is the dilution factor used at each transfer. For this experiment, the dilution factor D was set at 20. Consequently, lines cryopreserved after undergoing 52 transfers, resulted in a calculated generation number of $52 \times \log_2(20) \approx 225$. Similarly, lines harvested after 99 transfers had a generation number calculated as $99 \times \log_2(20) \approx 425$.

Thawed and evolving LNS lines were subjected to periodic conditions (12 h at 28°C, 220 µmol m^{-2} s^{-1} PPFD: 12 h at 18°C, dark) to synchronize the cultures before cell harvest, flow cytometry, and growth assays. The conditions for synchronization were ascertained by following the methodologies stipulated by Hlavová *et al.* (2016) and Angstenberger *et al.* (2020), supplemented with a process of laboratory trial and error. A summary of all experimental strains is given in Table 1. Once sufficient synchronization in the cell cycle was observed for all lines, as confirmed through microscopy, each experimental line was divided into six replicates, randomized, and cultivated for 3 d under the same conditions as in the LNS experiment and in the same incubator. Seventy-two hours post inoculation, 2 ml aliquots of each independent line was centrifuged to remove liquid culture, and the resulting samples were flash-frozen in liquid nitrogen. These samples were subsequently stored at −80°C until RNA extraction. Concurrently, an additional 1 ml sample was collected from each line for cell count (Multisizer 3 Coulter Counter).

Quantifying genome size

The determination of the genome size was performed by employing flow cytometry on propidium iodide (PI)-stained nuclei, according to the methodology outlined by Čertnerová & Galbraith (2021). Two milliliters of aliquot samples from all experimental strains was collected during the midexponential phase of a synchronized culture, specifically 2 h after the initiation of the light-warm phase, which corresponds to the early G1 phase. For each of the cell

cultures, the aliquot sample was centrifuged at 4000 ***g*** for 5 min, after which the excess growth medium was carefully removed to yield the pellet. Into a 2-ml Eppendorf tube, approximately ten 1.5-mm-diameter glass beads (Sigma-Aldrich) were introduced, along with 550 µl of ice-cold LB01 lysis buffer (Dpooležel *et al.*, 1989) and the harvested cell pellet. The cells were mechanically disrupted over a period of 3 min at a frequency of 25 Hz employing a Retsch MM400 mixer mill. The resulting lysate was then filtered through a 42 µm nylon mesh. The filtered sample was subsequently left to stand at room temperature for roughly 1 h, allowing for phase separation. Two distinct layers form: a lower green phase containing residual cell debris and pigments, and a colorless upper phase in which the nuclei are suspended. A 200-µl aliquot of this supernatant was carefully extracted and introduced to a staining solution composed of 550 µl of LB01 lysis buffer, 50 µg ml^{-1} PI, 50 µg ml^{-1} RNase IIA, and 2 µl ml^{-1} β-mercaptoethanol. Following an incubation period of roughly 10 min in the dark, flow cytometric analysis of these samples was conducted utilizing an Attune NxT Flow Cytometer instrument (Thermo Fisher Scientific, Waltham, MA, USA).

Fitness assays

Every experimental line was diluted to 1 : 25, taking it below the detection threshold of our plate reader, and divided into 12 replicates, which were randomly distributed onto 96-well plates (ref. 655 098, Greiner Bio-One, Kremsmünster, Austria). The optical density was measured approximately every 12 h over a span of 8 d using a VICTOR™ X Multilabel Plate Reader (PerkinElmer Inc., Waltham, MA, USA). We applied the Baranyi–Roberts equation to model growth curves, facilitating estimates of the maximum growth rate (MGR) (Baranyi & Roberts, 1994).

To detect significant differences in MGR among the experimental lines, we employed a strategy based on estimated marginal means (EMMs) and *post hoc* analysis. An analysis of variance (ANOVA) was conducted with the factors ploidy, line, and generation, along with their interaction terms, to model MGR. We assessed the normality of residuals using a QQ plot to ensure the assumptions of the ANOVA model were met. EMMs for all combinations of these factors were computed using the EMMEANS package in R, adjusting for other variables in the model. Pairwise comparisons of the estimated marginal means were performed using the Šidák correction to adjust for multiple comparisons and control the family-wise error rate.

RNA extraction and RNA-Seq

Total RNA was extracted using a Qiagen RNeasy® Plant Mini Kit and treated with RNase-free DNase (Qiagen). The assessment of total RNA quality and quantity was conducted utilizing a NanoDrop™ 2000c spectrophotometer (Thermo Fisher Scientific) and Bioanalyzer RNA6000 (Agilent Technologies). Library preparation and sequencing were conducted by the sequencing platform *NXTGNT* (http://www.nxtgnt.com/). cDNA libraries were generated using a QuantSeq™ 3′ mRNA-Seq library preparation kit (Lexogen, Vienna, Austria) in accordance with the manufacturer's guidelines. The 3′ RNA-Seq method offers comparable reproducibility to whole transcript analysis without transcript size bias, at a lower cost (Moll *et al.*, 2014). The Illumina NextSeq 500 was utilized for sequencing, yielding an average of 11.3M 76 bp single-end reads per sample (range: 8.7M–20.1M reads). Following Quality Control with FASTQC (Andrews, 2010), unique molecular identifiers (UMIs) were extracted using 'umi_tools extract' (Smith *et al.*, 2017), and the reads were trimmed utilizing 'bbduk' (Bushnell, 2014). Reads from identical libraries (processed in distinct runs and lanes) were amalgamated before 'hisat2' mapping (Kim *et al.*, 2019) onto the *C. reinhardtii* genome v.6 (Craig *et al.*, 2023). On average, 9M reads mapped one time to the reference genome (range: 6.9M–16.6M). PCR duplicates were eliminated by employing the UMIs and 'umi_tools dedup' (Smith *et al.*, 2017). Mapped reads were quantified using the PYTHON package HTSeq (Anders *et al.*, 2015).

Differential gene expression analysis

Differential expression (DE) analysis was performed with the BIOCONDUCTOR package *HybridExpress* on count data normalized by library size (Almeida-Silva *et al.*, 2024). This package facilitated the calculation of midparent values (MPV) for gene expression, exploratory data analysis, DEG analysis, gene categorization into different expression patterns (to be described later), and KEGG pathway overrepresentation analysis. Differential expression was determined using an adjusted *P*-value (Benjamini–Hochberg correction) threshold of $P < 0.01$. Differentially expressed genes were classified into categories and classes of expression patterns as developed by Rapp *et al.* (2009) and as implemented in the R package *HybridExpress*.

Inference and analysis of gene coexpression networks

Gene coexpression networks (GCNs) were inferred and analyzed with the BIOCONDUCTOR package BioNERO (Almeida-Silva & Venancio, 2022). Before network inference, count data were filtered to remove genes with less than one count in at least 50% of the samples, followed by variance-stabilizing transformation (Love *et al.*, 2014). We inferred a single GCN containing all samples, and five strain-specific GCNs containing only samples from the triploid ancestral line and evolved lines at generations 225 and 425. GCNs were inferred using biweight midcorrelations and the signed hybrid approach. Module preservation statistics were calculated using the NetRep method (Ritchie *et al.*, 2016) implemented in BioNERO, with 1000 permutations. Modules in the reference network (Line 1) were considered as preserved in other networks if at least five (of seven) preservation statistics were significant ($P < 0.05$).

Results

Genome merging slightly increases fitness and triploid lines show potential adaptation to experimental conditions

We assessed the fitness of experimental lines using a growth assay to measure MGR as a fitness proxy (Fig. 1). Detailed growth

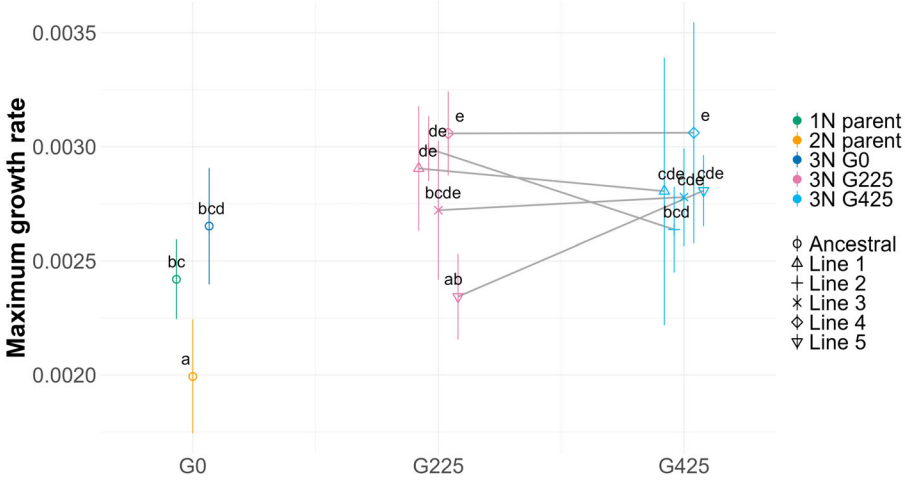

Fig. 1 Fitness assessment of experimental *Chlamydomonas reinhardtii* lines using maximum growth rate (MGR). Mean MGR of the experimental lines across three generations (G0, G225, and G425). Error bars represent SD. Statistical analysis was performed using ANOVA, followed by pairwise comparisons of estimated marginal means (EMMs) with Šidák correction for multiple comparisons. Different letters (a–e) indicate significant differences between groups ($P < 0.05$).

curves can be visualized in Fig. S1. The newly formed triploid (3N G0) showed significantly higher MGR than its diploid parent ($P < 0.001$, based on pairwise comparisons of EMMs with Šidák correction). The 3N G0 exhibited a higher MGR than its haploid parent as well, though the difference was not statistically significant. We also compared the MGR of evolved triploid lines at generation 225 (G225) with both the ancestral triploid (3N G0) and with these lines at G425 (Fig. 1). MGR of the five independent triploid lines were pooled and averaged by generations for comparison. We observed a slight increase in MGR from G0 to G225, followed by stabilization from G225 to G425 (Fig. S2).

Flow cytometry reveals rapid genome loss and stabilization in the triploids

Flow cytometry analyses were performed to determine the genome size of our experimental *C. reinhardtii* strains (Fig. S3). As expected, the haploid parental strain exhibited a genome size consistent with standard haploid *C. reinhardtii* strains, which was also verified with additional haploid control strains (mean fluorescence intensity (MFI) = 5692 (±673)). The diploid parent exhibited a genome size approximately twice that of the haploid strains, with an MFI of 11 914 (±1621), indicating diploidy – a ratio of *c.* 2.093 (±0.377) compared with the haploid MFI. This result was unexpected, as the strain was listed as haploid by the Chlamydomonas Resource Center at the time of acquisition. The diploid state of CC-1820 was independently confirmed three times using flow cytometry. Subsequently, the CC-1820 strain, alongside strain CC-1821, was reacquired from the Chlamydomonas Resource Center and flow cytometry analysis confirmed the diploid status in these strains.

Flow cytometry showed that the strain resulting from the cross of CC-1067 and CC-1820, followed by double complementation of the *arg* mutations, displayed a triploid state (MFI = 14 851(±2158)). This confirmed that this triploid progeny strain combined the chromosomal sets of CC-1067 and CC-1820. However, the genome size of the triploid progeny and the summed genome sizes of the parental strains (as measured by MFIs) are different. Indeed, with a combined parental MFI of 17 606 (±1755), the triploid progeny's genome size, representing *c.* 84.4% (±14.9%) of the parental genomes, indicates early-stage genome loss following genome merging.

Subsequently, the genome sizes of the evolved triploid lines were also measured by flow cytometry. Interestingly, every line seems to have undergone substantial genome loss within the first 225 generations. The MFI of the five independent lines was recorded as 13 634 (±1666) at generation 255. At G425, the MFI was 13 774 (±1825), indicating that after the initial drop genome size stabilizes fast (Fig. S3). The triploid genomes exhibited a reduction of *c.* 9% in size within 225 generations or less. When comparing the sum of the parental genomes, the theoretical reduction amounts to *c.* 22.3%.

Persistent and evolving gene expression in triploids across generations

Significant DE was detected between the two parental strains, with 6096 genes – *c.* 36.1% of the total gene count – being differentially expressed, using a *P*-value threshold of 0.01 (Fig. 2). Substantial DE levels were also evident between the parental strains and the initial triploid (3N G0), showcasing similar DEG proportions for the haploid and diploid parent, at 26.8% and 29.7%, respectively (Fig. 2a). 21.4% of genes demonstrated DE between the initial triploid and the MPV (Fig. 2a). A principal component analysis (PCA) of gene expression levels (Fig. 3) clearly separates the triploid derivative from the MPV and each parental strain, indicating distinct expression profiles. The analysis reveals that the triploid line does not manifest intermediate expression levels typical of parental additivity. Instead, it forms a well-defined cluster, distinct from both the parental strains and the MPV. Furthermore, while replicates within the same lineage number and LNS lines cluster tightly, G225 and G425 show no significant separation. However, LNS lines from G225 subtly tend to cluster closer to the ancestral state compared with those from G425.

Genes exhibiting DE between at least one pair within the trio – haploid parent, diploid parent, and triploid derivative – were classified into 12 expression patterns as delineated by

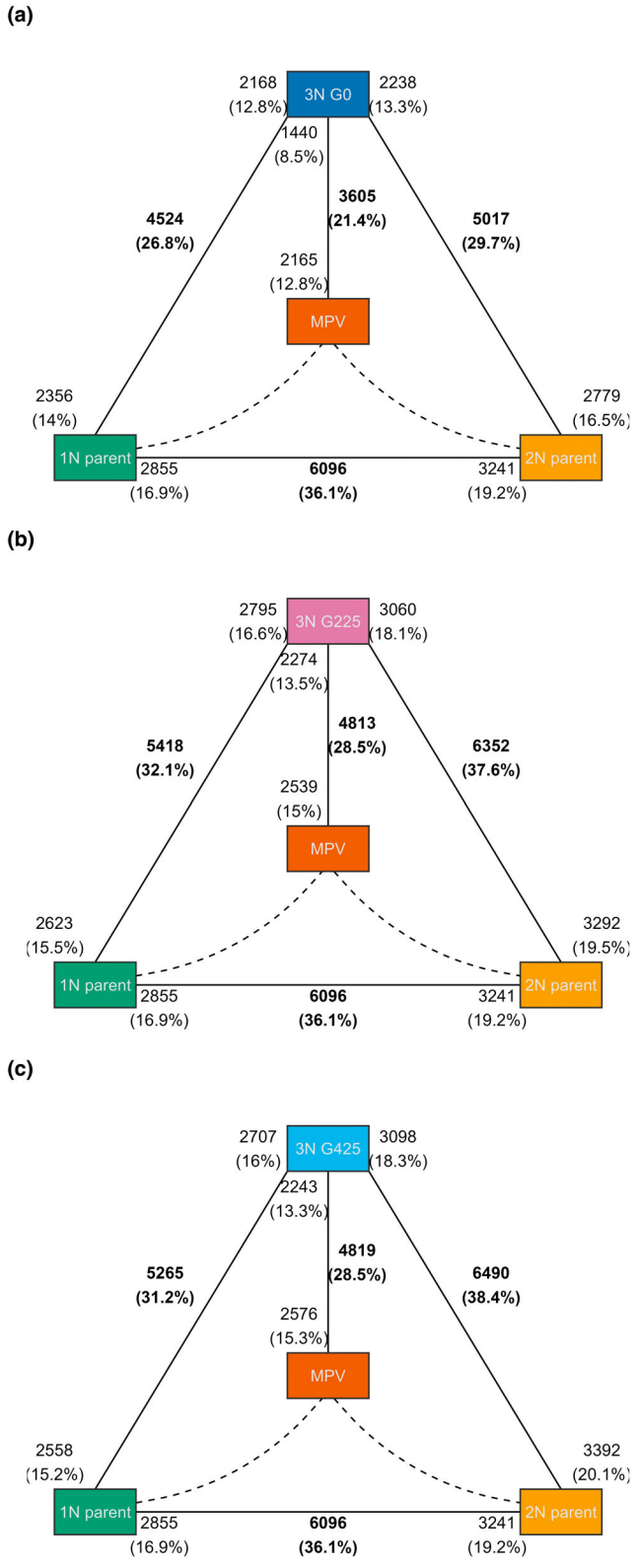

Fig. 2 Differential gene expression among *Chlamydomonas reinhardtii* ancestral parental strains and triploid lines. The haploid parent CC-1067 ('1N parent') is shown in green, the diploid parent CC-1820 ('2N parent') in orange, and the *in silico* midparent ('MPV'), representing the averaged expression profile of the two parents, in brown-orange. Each panel highlights the total number and percentage of differentially expressed genes in bold. Additionally, the direction of gene regulation – whether genes are upregulated in one group or another – is presented in regular (nonbold) text. For instance, in (a), 6096 genes are differentially expressed between the 1N and 2N parents, with 2855 genes upregulated in the 1N parent and 3241 genes upregulated in the 2N parent. (a) Comparisons with triploid progeny at generation 0 (3N G0). (b) Comparisons with triploid lines at generation 225 (3N G225). (c) Comparisons with triploid lines at generation 425 (3N G425).

Rapp *et al.* (2009) using the *HybridExpress* function *expression_partitioning* (Almeida-Silva *et al.*, 2024). These patterns were further grouped into five broad classes: transgressive upregulation (UP), transgressive downregulation (DOWN), additivity (ADDITIVE), ELD toward the haploid parent (ELD1), and ELD toward the diploid parent (ELD2). Gene expression pattern classification was applied to the ancestral triploid (G0), as well as collectively across the five independently evolving triploid lines at G225 and G425 (Fig. 4). By pooling the data from these lines, we aimed to identify expression patterns indicative of selective pressures, thereby minimizing the potential confounding effects of genetic drift. Consistent with preceding DE results, only 3.57% (603) of the DEGs showed additive expression at G0, exhibiting levels intermediate between the parental strains. This number rose to *c.* 6.5% at both G225 and G425 (1094 and 1093, respectively). Transgressive expression constituted a substantial fraction of DEGs, comprising 3.39% (572) of upregulated genes and 5.17% (873) of downregulated genes at G0. Upregulated gene numbers increased to *c.* 5% at both G225 and G425 (852 and 854, respectively). The downregulated gene fraction slightly decreased with 5.64% (953) and 5.8% (980) genes at G225 and G425, respectively. Remarkably, at G0, *c.* 25% (4150 genes) of DEGs showed ELD. At G0, genes showing ELD1 and ELD2 were at proportions of 13.3% (2245) and 11.28% (1905), respectively. The number of ELD1 genes increased from 2245 at G0, to 2416 at G225, and finally to 2478 at G425. ELD2 genes declined to 10.41% (1758) and 9.81% (1656) at G225 and G425, respectively.

A notably high proportion of genes share constant expression patterns across three generations, particularly for ELD, ranging from 26% for genes consistently upregulated to 45% for genes exhibiting ELD1. These genes, maintaining consistent class categorization across generations, are henceforth termed 'persistent genes' (Fig. S4).

To follow the evolution of expression level after genome merging, genes that showed DE between at least one pair within the trio – ancestral triploid (3N G0), triploid LNS lines at G225 (3N G225), and triploid LNS lines at G425 (3N G425) – were sorted into the analogous 12 expression patterns employed for the three ancestral strains in the preceding analysis (Fig. 5). This approach enabled the identification of any significant changes in expression levels throughout the duration of the LNS experiment. A total of 1040 genes demonstrated DE between at least one of the comparisons while 15 843 genes showed no DE. A substantial

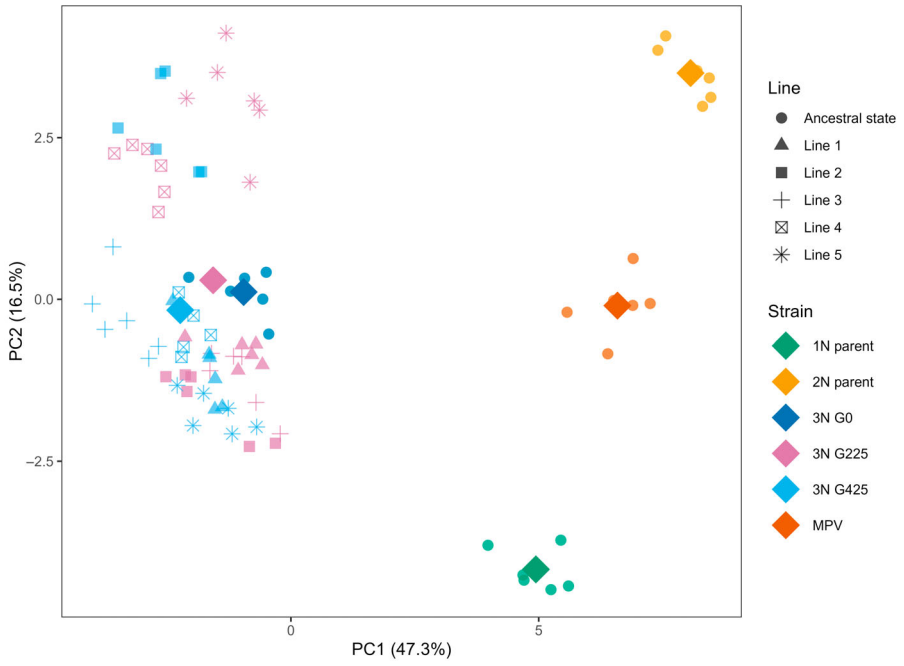

Fig. 3 Principal component analysis of differential expression levels in *Chlamydomonas reinhardtii* experimental lines. Each individual replicate is depicted by a small, slightly transparent dot, with the shape varying according to the associated line. Group aggregates are denoted by larger, opaque rhombus symbols. The ancestral strains, comprising the haploid parent, the diploid parent, the triploid derivative, and the midparent values (MPV), are distinguished by color codes: green, orange, purple, and brown-orange, respectively. Evolved triploids are illustrated using distinct shapes, contingent on the lines, and unique colors, contingent on the generation: generation 225 is represented in salmon pink, while generation 425 is delineated in blue.

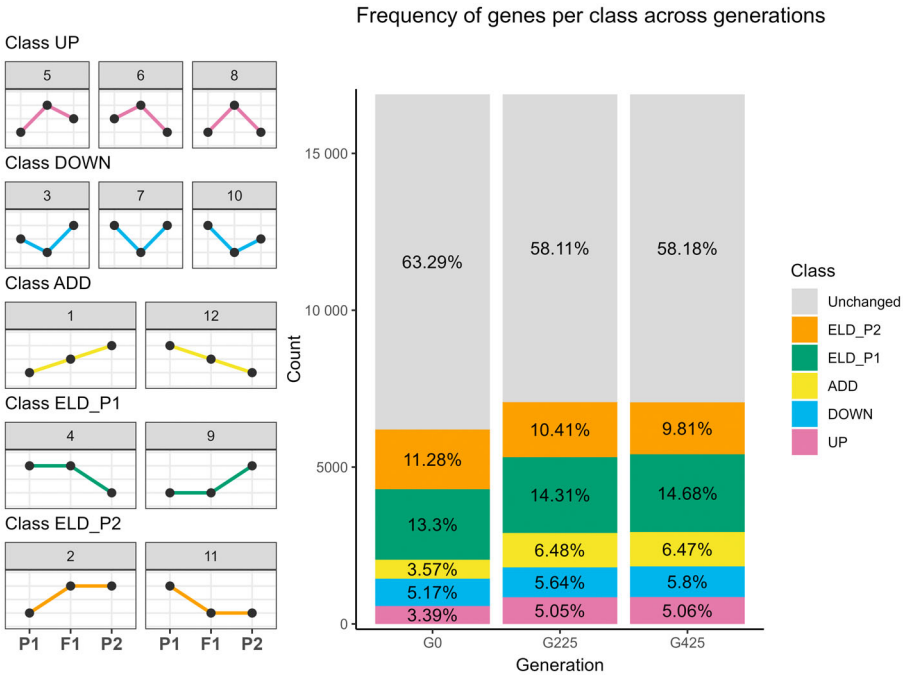

Fig. 4 Partitioning of expression patterns in the *Chlamydomonas reinhardtii* triploid derivative in relation to its haploid and diploid progenitors at generation 0 (G0), generation 225 (G225), and generation 425 (G425). The differentially expressed genes are binned in five distinct expression patterns: transgressive upregulation (UP, in red), transgressive downregulation (DOWN, in blue), additivity (ADD, in gold), expression level dominance toward the haploid parent (ELD_P1, in green), and expression-level dominance toward the diploid parent (ELD_P2, in orange). Left: graphical representations detailing the 12 potential expression patterns observed between the two parental strains and their derivative, binned in five groups (P1, haploid parent; F1, triploid derivative; P2, diploid parent); Right: stacked bar plots showing the number and fraction of differentially expressed genes that fall in the five possible expression patterns in the triploid at G0, G225, and G425 (from left to right).

81.7% of the DEGs fell into categories 2, 11, 7, and 8, leaving the remaining eight categories with considerably fewer genes. Categories 2 and 11 (286 and 159 genes, respectively) corresponded to genes that underwent significant changes in expression levels within the initial 225 generations, subsequently stabilizing. Categories 7 and 8 (175 and 230 genes, respectively) corresponded to genes that manifested similar expression levels between G0 and G425, but significantly different expression at G225.

Enrichment analysis reveals immediate and evolutionary consequences to genome merging in gene expression

We examined enrichment of KEGG metabolic pathways in genes classified in the five expression patterns observed consistently at G0, G225, and G425, termed 'persistent genes' (Fig. S4). Upregulated genes (UP) demonstrated no significant enrichment in any metabolic pathways. Conversely, downregulated genes (DOWN) exhibited substantial enrichment, particularly in

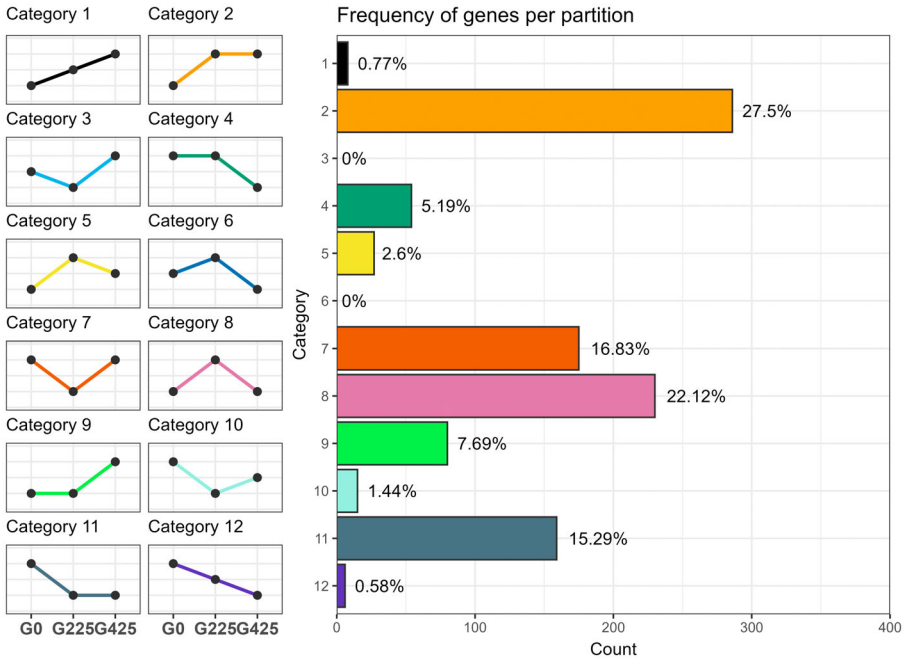

Fig. 5 Partitioning of patterns of expression level evolution in the *Chlamydomonas reinhardtii* triploid lines. Left: graphical representations detailing the 12 possible expression categories observed between the three generations (G0, G225, and G425) of the triploid lines; Right: bar plots showing the number and fraction of differentially expressed genes that fall in the 12 possible categories (right). In addition to the DE genes, 15 843 genes did not exhibit differential expression and are not represented in these categories.

KEGG pathways associated with the chloroplast and mitochondria, including 'Photosynthesis' and the 'Krebs cycle' (Table S1). Additive genes (ADD) showed no pathway enrichment overall. ELD1 genes were primarily enriched in pathways related to ribosomes and the metabolism of proteins and amino acids, as outlined in Table S2. Similar to the UP and ADD classes, ELD2 genes displayed no significant pathway enrichment.

We also analyzed the overrepresentation of Gene Ontology (GO) terms in genes within the different categories of evolution (Fig. 5). Among the 12 categories, only Categories 2 and 11 showed significant enrichment. Category 2, which includes genes that showed a rapid increase in expression levels during the experiment, displayed enrichment in terms associated with 'autophagy' and 'protein catabolic process' (Table S3). Category 11, representing genes that experienced a rapid decrease in expression, showed enrichment in 'translation' and 'peptide biosynthetic process' (Table S4). This suggested an evolution of the peptide anabolism and catabolism processes in the triploid lines, potentially caused by an initial disruption after genome merging. To investigate this, we examined KEGG pathway enrichment in DOWN and UP genes in the ancestral triploid at G0. Notably, UP genes showed significant enrichment in 'Ribosome biogenesis in eukaryotes', while DOWN genes showed significant enrichment in 'Proteasome', indicative of a disruption of proteostasis following genome merging.

Gene coexpression networks reveal temporal changes in biological processes

We inferred a gene coexpression network (GCN) with all samples using BioNERO (Almeida-Silva & Venancio, 2022) and identified 62 modules, of which 15 were enriched in genes associated with GO terms and/or KEGG pathways (Figs 6a, S5). As per BioNERO's default behavior, coexpression modules are represented by different color names. Module *blue* contained genes involved in the biosynthesis of secondary metabolites and carbon metabolism, with decreased expression levels in triploid G0 (Fig. 6b). Genes in modules *blue2* and *darkseagreen3* were associated with response to osmotic stress, and noncoding RNAs (ncRNA processing, gene silencing by miRNAs, and histone methylation), respectively, and their expression in triploid G0 corresponded to the mean of the 1N and 2N parents (Fig. 6b). Genes in module *darkgreen* were involved in cell cycle and displayed dramatically lower expression levels in the 1N parent and triploid G0. Module *darkslateblue* contained genes involved in rRNA maturation and regulation of ribosome biogenesis, and they displayed increased expression levels in triploid G0, with ever-increasing expression levels over time in evolved lines.

Further, we hypothesized whether there is an association between a gene's expression-based class (i.e. UP, DOWN, ADD, ELD1, and ELD2; as mentioned in the previous sections) and its degree in the GCN (i.e. sum of all edge weights). We observed that genes in classes UP, DOWN, and ADD were overrepresented in hubs ($P < 0.001$). Based on numerous reports on the association between hub genes and essentiality in a cell, with hub gene knockouts leading embryo lethality (Jeong *et al.*, 2001; Yu *et al.*, 2004; Zotenko *et al.*, 2008; Song *et al.*, 2015; Almeida-Silva *et al.*, 2020), this finding suggests that genes in these classes have a more prominent role in the organism's fitness.

Most genes displayed preserved expression levels across different evolved lines

We observed some variation in expression levels across different lines within the same generation (Fig. 6b). To test whether

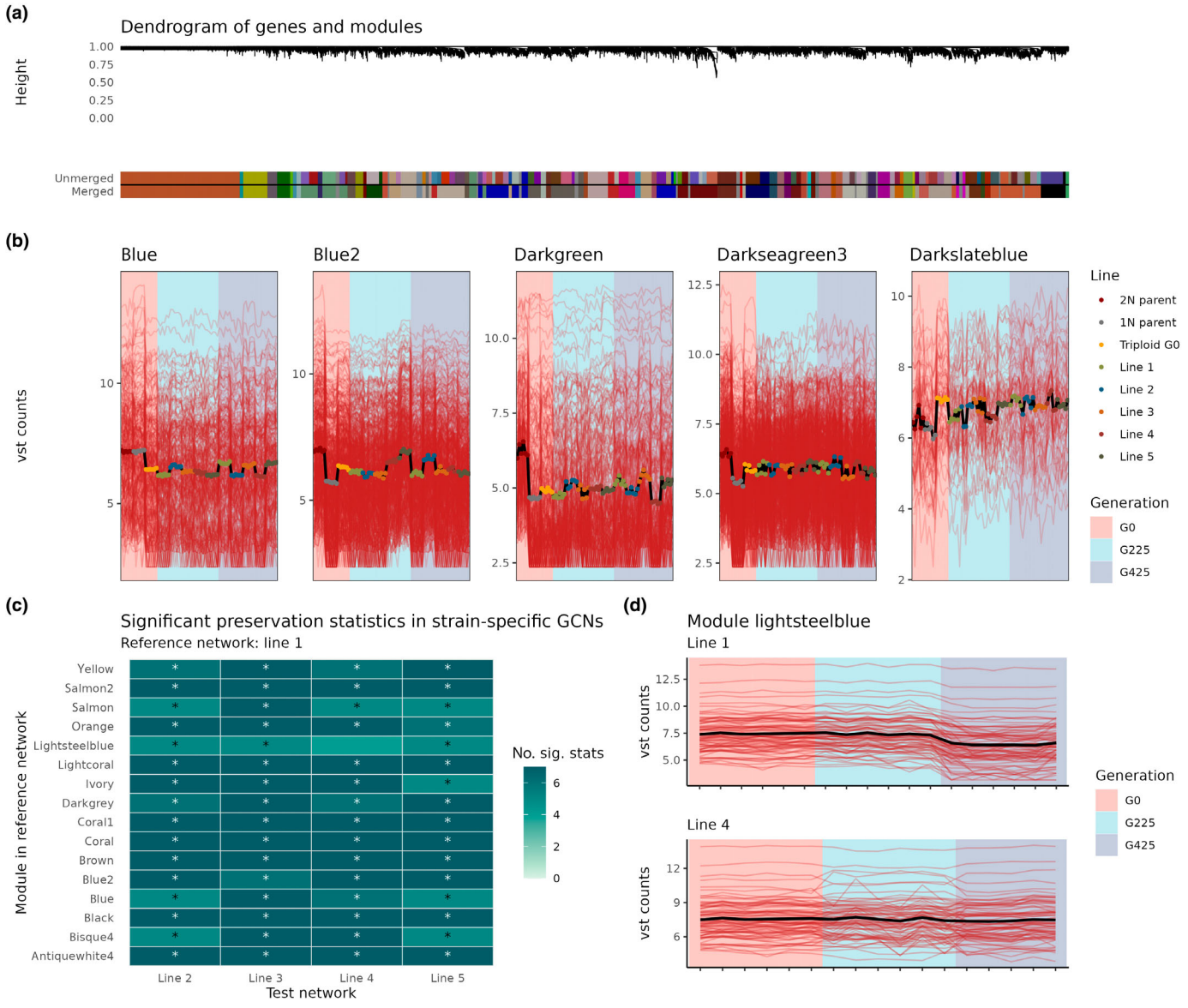

Fig. 6 Gene coexpression network analyses in the *Chlamydomonas reinhardtii* lines. (a) Dendrogram of genes and modules obtained with BioNERO. Modules with correlations between eigengenes > 0.8 were merged into a single larger module to remove redundancy. (b) Expression profiles of selected modules enriched in functional terms (Gene Ontology and/or KEGG pathways). Expression levels are represented as variance-stabilized count data (i.e. vst counts). (c) Significant network preservation statistics between reference and test strain-specific coexpression networks (GCNs). Statistics were obtained by comparing modules in the reference strain-specific gene coexpression network (line 1) with all other strain-specific networks. All preservation statistics in the NetRep algorithm were used. Asterisks indicate modules that had at least five significant preservation statistics. (d) Expression profiles of the genes in module *lightsteelblue* (reference network) in lines 1 and 4. The module *lightsteelblue* was the only module in the reference network that was not preserved in other test networks. The line plots indicate that expression divergence between Line 1 and Line 4 occurs after generation 425.

different lines had divergent expression profiles over generations, we inferred GCNs separately for each line (hereafter referred to as 'strain-specific GCNs' or 'ssGCNs'). We then calculated module preservation statistics between a reference ssGCN (for Line 1) and all other test ssGCNs (Lines 2, 3, 4, and 5) using preservation statistics implemented in the NetRep algorithm (see Materials and Methods section for details). We observed that all modules in the reference ssGCN were preserved in the ssGCNs for nearly all test ssGCNs, except for module *lightsteelblue* in the ssGCN for Line 4 (Fig. 6c). After further investigation, we found that divergence in expression profiles between Lines 1 and 4 occurred after generation 425 (Fig. 6d), with a decrease in expression levels in Line 1, but not in Line 4. A list of the genes in the module *lightsteelblue* can be found in Table S5. Functional enrichment analyses revealed no enriched terms for genes in module *lightsteelblue*. Yet, we note the presence of a few genes with important biological function such as RuBisCO (Cre02.g120150) in this list.

Discussion

Asymmetric genome merging causes transcriptomic shock

Genome merger can produce gene expression patterns that show intermediate levels of the parent species, as suggested by the additivity hypothesis (Buggs *et al.*, 2014; Yoo *et al.*, 2014). Indeed, many homoploid hybrids and allopolyploids exhibit predominantly additive gene expression relative to their parents (Chelaifa *et al.*, 2013; Zhang *et al.*, 2016; Bartoš *et al.*, 2019; Zhou *et al.*, 2019). However, examples of 'transcriptomic shock', characterized by extensive nonadditive gene expression, are also well-documented (Hegarty *et al.*, 2006; Wang *et al.*, 2006; Flagel & Wendel, 2010; Wu *et al.*, 2018; Li *et al.*, 2020). Such shocks lead to novel expression patterns, introducing phenotypic variations that could drive adaptation (Mable, 2013; Van de Peer *et al.*, 2021).

Our RNA-Seq experiment uncovered a pronounced transcriptomic shock in our newly formed triploid *C. reinhardtii* line, characterized by large differences in gene expression and unique gene expression patterns. The extent of this shock is surprising, as it typically occurs when genomes from different species are merged, whereas in this case, the genomes of two strains from the same species were combined. However, the parental strains, despite belonging to the same species, exhibited substantial differences in gene expression (Fig. 2), which might explain the unexpected shock observed in the triploid (Zhang *et al.*, 2019). This marked discrepancy in expression might be attributed to the differing ploidy levels (haploid vs diploid) and haplotype differences. We note that mutations could have disrupted the expression patterns of the diploid, as this strain was exposed to a mutagenic agent that potentially caused its diploidization (Loppes, 1969). The transcriptomic shock in the triploid appears to have occurred immediately following genome merging, as evidenced by its presence in the ancestral triploid strain (G0), and it has persisted over 425 subsequent generations. Although variation exists, both the patterns of gene expression and the specific genes involved showed a tendency for inheritance (Figs 4, S4), contrasting with previous results in newly formed allohexaploid wheat (Qi *et al.*, 2012). These results provide a compelling example of novel and heritable expression patterns emerging very rapidly after genome merging within a single sexual generation. Interestingly, the triploid lines showed an increase in fitness, approximated by MGR, compared with both parental strains, though only significant for the diploid parent (Figs 1, S2). This suggests that the observed transcriptomic shock, rather than detrimentally affecting fitness, potentially contributed to increase it under our laboratory conditions.

Complex parental legacy observed in the triploid lines

Strong gene-level dominance was evident, as approximately two-thirds of the DE genes exhibited ELD toward either the haploid or the diploid parent. Notably, despite asymmetric genome inheritance, the triploid progeny did not exhibit genome-wide dominance favoring the diploid parent (i.e. ELD2). Moreover, the number of genes demonstrating ELD1 slightly outnumbered those showing ELD2 at G0. This bias toward the haploid parent appeared to intensify in subsequent generations (Fig. 4), suggesting a potential ongoing parental dominance from the haploid strain.

Additionally, the overrepresentation analyses of the ELD1 and ELD2 gene sets revealed a distinct contrast in biological roles. Specifically, ELD1 genes were enriched in five KEGG pathways, predominantly those involved in amino acid metabolism, whereas ELD2 genes did not show enrichment in any pathway. Considering these observations – the increasing proportion of ELD1 genes relative to ELD2 genes, the similar fitness levels of the triploid and the haploid parent, and the results of the enrichment analysis – we conclude that the triploid potentially exhibits functional dominance toward its haploid parent, despite the unfavorable imbalanced genome inheritance. It is conceivable that this haploid dominance could be due to the higher fitness of the haploid parent relative to the diploid parent in our laboratory conditions (Fig. 1). Indeed, during the LNS experiment, these fitness advantages could have led to a selective pressure favoring traits associated with the haploid genome. Consequently, the prevalence of haploid dominance in the triploid could be an adaptive response, optimizing the triploid's metabolism to enhance growth under our experimental conditions. Concurrently, biased genome loss may also contribute to this observed haploid dominance. Flow cytometry data indicate a rapid reduction in genome size during the LNS within the triploid lines (Fig. S3). If this genome loss disproportionately affects the diploid parent's genome, it could further explain the persistence of haploid dominance. However, this remains speculative, and genome sequencing will be required to confirm any bias in genome fractionation toward the diploid genome.

These results align with numerous prior studies showing that allopolyploids often exhibit dominance at the gene expression levels toward one of the parental species (Rapp *et al.*, 2009; Li *et al.*, 2020; Glombik *et al.*, 2021). This phenomenon has been extensively reviewed in the literature, highlighting its prevalence and significance in allopolyploid evolution (De Smet & Van de Peer, 2012; Grover *et al.*, 2012; Buggs *et al.*, 2014; Yoo *et al.*, 2014; Wendel *et al.*, 2018). However, the observation that the dominant genome is haploid rather than diploid presents a surprising deviation from previous studies on resynthesized allohexaploid wheat, which predominantly demonstrated a dosage effect influencing expression level dominance (Qi *et al.*, 2012; Li *et al.*, 2014). This deviation could be influenced by external conditions, which significantly affect the parental legacy of gene expression in allopolyploids (Bardil *et al.*, 2011; Shimizu-Inatsugi *et al.*, 2017). Although our strains were cultivated under optimal conditions, the observed 'haploid functional dominance' may be due to the superior fitness of the haploid parent in these specific conditions. Further experimentation including genome and epigenome sequencing is needed to confirm these findings and to explore the underlying mechanisms of this dominance.

Asymmetric genome merging leads to major disruptions of cytonuclear stoichiometry and proteostasis

Enrichment of KEGG pathways and GO term gave insights into the consequences of genome merging for the cell biology of the new triploid strain. The significant presence of KEGG pathways linked to photosynthesis and carbon metabolism in downregulated genes suggested a disruption of the cytonuclear stoichiometry in the triploid (Table S1). Additionally, our coexpression analysis shows that the module *blue* containing genes involved in carbon metabolism displayed decreased expression level in triploid G0. Given the potential disruptive effect of ploidy change on the stoichiometry of the three plant cell genomes (Sharbrough *et al.*, 2017; Doyle & Coate, 2019), we hypothesize that these enrichment outcomes were caused by a change of the relative copy number of nuclear, mitochondrial, and plastid genomes in the triploid. Following the increase in nuclear genome copy numbers, compensatory mechanisms may help maintain cytonuclear stoichiometry. Sharbrough *et al.* (2017) proposed reduced nuclear gene expression per genome copy as one such mechanism. We suggest that the triploid lines downregulated nuclear organellar-targeted genes in response to fewer organellar genomes per nuclear genome. This hypothesis will be further explored in a follow-up genomic study.

This finding is surprising, as *C. reinhardtii* typically increases its chloroplast DNA content with ploidy level (Whiteway & Lee, 1977), a trend also observed in *Arabidopsis* autopolyploids (Coate *et al.*, 2020; Fernandes Gyorfy *et al.*, 2021). However, it is important to note that while Whiteway & Lee (1977) tested diploid strains, our study focuses on triploid strains. This distinction is significant because *C. reinhardtii* does not naturally exhibit a triploid stage in its life cycle, potentially influencing chloroplast DNA regulation in ways not observed in diploids. Additionally, unlike angiosperms such as *Arabidopsis*, which typically do not downregulate organelle-targeted genes to compensate for altered cytonuclear stoichiometry – due to their ability to upregulate organelle DNA replication to solve stoichiometric imbalance – *C. reinhardtii* lacks such evolutionary history of polyploidy. WGDs are comparatively rare in algae compared with angiosperms (Leebens-Mack *et al.*, 2019), which may explain the difference in mechanism modulating cytonuclear balance under increased ploidy levels. These results offer important insights for comparing how different green-plant lineages, shaped by their distinct evolutionary histories, compensate for cytonuclear disruptions, which can inform broader hypotheses on the regulation of organelle genomes. For instance, Li *et al.* (2020) observed a downregulation in photosynthesis-related pathways in natural allotetraploid *Brassica napus*, aligning with our findings. Contrarily, numerous studies report an increase in photosynthetic rates, chloroplast density, and Chl content in both established and newly synthesized allopolyploids (Warner & Edwards, 1993; Vyas *et al.*, 2007; Coate *et al.*, 2012; Ilut *et al.*, 2012). Additionally, Coate & Doyle (2013) noted increased expression of certain photosynthesis-related genes, while Forsythe *et al.* (2022) found that established polyploid plants preserved cytonuclear expression ratios, demonstrating their capacity to adapt to cytonuclear disruptions. Similarly, newly formed autotetraploids of *Festuca pratensis* and *Lolium multiflorum*, induced by colchicine, increased their chloroplast and chloroplast genome copy numbers by approximately twofold to compensate for disrupted cytonuclear stoichiometry, with no significant differences in nuclear or chloroplast gene expression levels (Shahbazi *et al.*, 2024). These contrasting observations underscore the complex effects that genome merging and doubling may have on cytonuclear stoichiometry and/or the regulation of photosynthesis genes (Grover *et al.*, 2022).

Although normal mating processes predominantly result in maternal inheritance (*mt*+) of chloroplasts (Burton *et al.*, 1979; Kuroiwa *et al.*, 1982) and paternal inheritance (*mt*−) of mitochondria (Nakamura, 2010), the inheritance patterns of the organellar genomes in our triploid remain unclear. This is particularly relevant for our triploid strains, as they have not undergone zygospore formation, making the inheritance patterns of chloroplasts even more unpredictable (Gillham, 1969). Future genomic sequencing and analysis will be crucial to elucidate these patterns.

Growth assay results (Figs 1, S2) indicate increased MGR despite the cytonuclear disruption under optimal growing conditions. Similarly, GO enrichment of genes with significant expression changes after genome merging do not suggest any adaptation to this new cytonuclear stoichiometry, such as increased expression of organellar genes (Tables S3, S4). This resilience aligns with recent findings on the robustness of cytonuclear interactions following disruptions in allopolyploid angiosperms (Sloan *et al.*, 2024). The minimal impact on fitness could also be attributed to the use of TAP medium, which contains acetate – a carbon source that *C. reinhardtii* can metabolize heterotrophically – possibly mitigating the effects of this disruption on growth (Heifetz *et al.*, 2000).

The genome merging in the triploid strain notably led to a downregulation of genes involved in protein degradation and an upregulation of those linked to protein biosynthesis, indicating an initial disruption of protein homeostasis (proteostasis). Gene expression analysis postmerging revealed a distinct pattern: significant early changes (between G0 and G225) that later stabilized (between G225 and G425; Fig. 5). GO enrichment analysis indicated that genes which rapidly decreased in expression were primarily associated with protein biosynthesis (Table S4), whereas genes with increased expression were linked to protein catabolism (Table S3). These findings suggest that the evolution of gene expression in the triploid lines was predominantly driven by selection pressures aimed at restoring proteostasis. As shown in yeast (Lu *et al.*, 2016), excessive protein production appears to be a major intrinsic stress of neopolyploidization, suggesting that restoring proteostasis is a crucial adaptation to polyploidy. However, our understanding of the impact of polyploidy on the proteome remains limited, necessitating further research to fully explore its effects (Soltis *et al.*, 2016; Doyle & Coate, 2019).

Genome downsizing in the triploid lines

Genome instability and downsizing as we observed in our polyploid Chlamydomonas lines seems to be common features of

polyploid organisms. Similar observations have been made with other eukaryotic unicellular species, such as *Saccharomyces cerevisiae* (Gerstein *et al.*, 2006; Storchova, 2014), *Candida albicans* (Bennett & Johnson, 2003; Hickman *et al.*, 2015), *Cryptococcus neoformans* (Gerstein *et al.*, 2015), and *Candida tropicalis* (Seervai *et al.*, 2013). Furthermore, genome instability has been observed in many neopolyploid angiosperm species (Raina *et al.*, 1994; Song *et al.*, 1995; Ma & Gustafson, 2005; Mestiri *et al.*, 2010; Xiong *et al.*, 2011; Buggs *et al.*, 2012; Chester *et al.*, 2012; Zhang *et al.*, 2013; Gou *et al.*, 2018; Li *et al.*, 2021; Lv *et al.*, 2022) and human solid tumors (Storchova & Pellman, 2004; Ganem *et al.*, 2007; Thompson & Compton, 2008; Thompson *et al.*, 2010), underscoring the potential universality of this phenomenon in eukaryotes.

Several mechanisms may contribute to the genome downsizing observed in the polyploid Chlamydomonas strains. The euploid history hypothesis suggests adaptation to a certain genome/cell size, optimizing cellular function (Storchova, 2014). This hypothesis has been used to explain diploidization in yeast (Storchova, 2014); however, conversely to yeast, Chlamydomonas' life cycle is predominantly haploid during its metabolically active phase, while containing a diploid phase as a zygospore. Moreover, we did not observe a complete diploidization in the triploid lines but a loss of *c.* 22.3% of the genome. Factors such as nutrient and energy efficiency, as well as selection for higher growth rate, may also have driven genome size reduction (Hessen *et al.*, 2010; Malerba *et al.*, 2020; Wang *et al.*, 2021). Additionally, larger cells have shown decreased photosynthetic efficiency due to the 'package effect' (Malerba *et al.*, 2018); selection for more efficient photosynthesis in smaller cells may inadvertently favor smaller genomes. As an additional mechanism, we propose that the restoration of cytonuclear stoichiometry could have also driven genome downsizing (Sharbrough *et al.*, 2017), yet this could be seen as a component of the euploid history hypothesis (Storchova, 2014), and this was not observed in the gene expression data. To further understand the underlying mechanisms driving this reduction, we plan to perform detailed genome sequencing analyses. This approach will help elucidate the specific genomic changes involved.

Concluding remarks

Our study leverages *C. reinhardtii*, a unicellular green alga closely related to angiosperms, as a unique model to explore the cellular and evolutionary implications of polyploidy (Bafort *et al.*, 2023). This system allows for detailed examination of both the immediate cellular responses and the longer term evolutionary impacts of genome merging. In our study of newly formed triploid *C. reinhardtii* strains, RNA-Seq and flow cytometry results revealed significant transcriptomic and potential proteomic and genomic shocks, accompanied by disruptions in cytonuclear stoichiometry. Future studies focusing on the genomic changes occurring within these triploid lines will shed light into the potential molecular mechanisms, such as structural variation, genome fractionation, chromosomal instability, and epigenetic modifications, providing deeper insights into the consequences of polyploidy.

Acknowledgements

The authors thank Dr Eylem Aydogdu for helping set up the Chlamydomonas system. We also thank Dr Marlies Peeters and Dr Zhen Li for their insightful discussions, as well as the two reviewers for their helpful comments. YVdP acknowledges funding from the European Research Council (ERC) under the European Union's Horizon 2020 research and innovation program (Grant No. 833522). YVdP and ODC received funding from the Fonds Wetenschappelijk Onderzoek (FWO Research Project – G0C0116N) and infrastructure grant (EMBRC Belgium, FWO ESFRI – I001621N). AVdV and FA-S were funded by Ghent University (Methusalem funding, BOF.MET.2021.0005.01). LP-B and QB were awarded PhD scholarships by the Fonds Wetenschappelijk Onderzoek (FWO) of Flanders (grant nos. 11H0426N and 1168420N, respectively).

Competing interests

None declared.

Author contributions

LP-B was involved in conceptualization (lead), formal analysis (lead), investigation (equal), writing – original draft (lead), writing – review and editing (equal), and visualization (lead). QB was involved in conceptualization (supporting), and writing – review and editing (equal). AVdV was involved in investigation (supporting), formal analysis (supporting), writing – original draft (supporting) and writing – review and editing (equal). FA-S was involved in formal analysis (supporting), visualization (supporting), writing – original draft (supporting) and writing – review and editing (equal). YTP, GC and SD were involved in investigation (equal). ODC was involved in conceptualization (supporting), supervision (equal) and writing – review and editing (equal). YVdP was involved in conceptualization (supporting), supervision (equal), funding acquisition (lead) and writing – review and editing (equal).

ORCID

Fabricio Almeida-Silva https://orcid.org/0000-0002-5314-2964
Quinten Bafort https://orcid.org/0000-0003-2155-3344
Griet Casteleyn https://orcid.org/0000-0002-3386-1865
Sofie D'hondt https://orcid.org/0000-0002-2128-0553
Olivier De Clerck https://orcid.org/0000-0002-3699-8402
Yunn Thet Paing https://orcid.org/0009-0007-5665-9911
Lucas Prost-Boxoen https://orcid.org/0000-0003-2779-9097
Yves Van de Peer https://orcid.org/0000-0003-4327-3730
Antoine Van de Vloet https://orcid.org/0000-0002-6967-9168

Data availability

The RNA-Seq 3′ QuantSeq data generated in this study are available in the NCBI Sequence Read Archive (SRA) under the accession no. PRJNA1145893.

References

Adams K, Wendel J. 2005. Novel patterns of gene expression in polyploid plants. *Trends in Genetics* **21**: 539–543.

Adams KL, Cronn R, Percifield R, Wendel JF. 2003. Genes duplicated by polyploidy show unequal contributions to the transcriptome and organ-specific reciprocal silencing. *Proceedings of the National Academy of Sciences, USA* **100**: 4649–4654.

Albertin W, Marullo P. 2012. Polyploidy in fungi: evolution after whole-genome duplication. *Proceedings of the Royal Society B: Biological Sciences* **279**: 2497–2509.

Almeida-Silva F, Moharana KC, Machado FB, Venancio TM. 2020. Exploring the complexity of soybean (*Glycine max*) transcriptional regulation using global gene co-expression networks. *Planta* **252**: 104.

Almeida-Silva F, Prost-Boxoen L, de Peer YV. 2024. HybridExpress: an R/bioconductor package for comparative transcriptomic analyses of hybrids and their progenitors. *New Phtologist* **243**: 811–819.

Almeida-Silva F, Venancio TM. 2022. BioNERO: an all-in-one R/bioconductor package for comprehensive and easy biological network reconstruction. *Functional & Integrative Genomics* **22**: 131–136.

Anders S, Pyl PT, Huber W. 2015. HTSeq—a Python framework to work with high-throughput sequencing data. *Bioinformatics* **31**: 166–169.

Andrews S. 2010. FastQC: a quality control tool for high throughput sequence data. [WWW document] URL http://www.bioinformatics.babraham.ac.uk/projects/fastqc/.

Angstenberger M, de Signori F, Vecchi V, Dall'Osto L, Bassi R. 2020. Cell synchronization enhances nuclear transformation and genome editing via Cas9 enabling homologous recombination in *Chlamydomonas reinhardtii*. *ACS Synthetic Biology* **9**: 2840–2850.

Auger DL, Gray AD, Ream TS, Kato A, Coe EH Jr, Birchler JA. 2005. Nonadditive gene expression in diploid and triploid hybrids of maize. *Genetics* **169**: 389–397.

Bafort Q, Prost L, Aydogdu E, Van de Vloet A, Casteleyn G, Van de Peer Y, De Clerck O. 2023. Studying whole-genome duplication using experimental evolution of Chlamydomonas. In: Van de Peer Y, ed. *Methods in molecular biology. Polyploidy: methods and protocols*. New York, NY, USA: Springer US, 351–372.

Baranyi J, Roberts TA. 1994. A dynamic approach to predicting bacterial growth in food. *International Journal of Food Microbiology* **23**: 277–294.

Bardil A, Almeida JD d, Combes MC, Lashermes P, Bertrand B. 2011. Genomic expression dominance in the natural allopolyploid Coffea arabica is massively affected by growth temperature. *New Phytologist* **192**: 760–774.

Bartoš O, Röslein J, Kotusz J, Paces J, Pekárik L, Petrtýl M, Halačka K, Štefková Kašparová E, Mendel J, Boroń A *et al.* 2019. The legacy of sexual ancestors in phenotypic variability, gene expression, and homoeolog regulation of asexual hybrids and polyploids. *Molecular Biology and Evolution* **36**: 1902–1920.

te Beest M, Le Roux JJ, Richardson DM, Brysting AK, Suda J, Kubešová M, Pyšek P. 2012. The more the better? The role of polyploidy in facilitating plant invasions. *Annals of Botany* **109**: 19–45.

Behling AH, Winter DJ, Ganley ARD, Cox MP. 2022. Cross-kingdom transcriptomic trends in the evolution of hybrid gene expression. *Journal of Evolutionary Biology* **35**: 1126–1137.

Bell GAC. 1997. Experimental evolution in Chlamydomonas. I. Short-term selection in uniform and diverse environments. *Heredity* **78**: 490–497.

Bennett RJ, Johnson AD. 2003. Completion of a parasexual cycle in *Candida albicans* by induced chromosome loss in tetraploid strains. *EMBO Journal* **22**: 2505–2515.

Bird KA, VanBuren R, Puzey JR, Edger PP. 2018. The causes and consequences of subgenome dominance in hybrids and recent polyploids. *New Phytologist* **220**: 87–93.

Bomblies K. 2020. When everything changes at once: finding a new normal after genome duplication. *Proceedings of the Royal Society B: Biological Sciences* **287**: 20202154.

Buggs RJA, Chamala S, Wu W, Tate JA, Schnable PS, Soltis DE, Soltis PS, Barbazuk WB. 2012. Rapid, repeated, and clustered loss of duplicate genes in allopolyploid plant populations of independent origin. *Current Biology* **22**: 248–252.

Buggs RJA, Wendel JF, Doyle JJ, Soltis DE, Soltis PS, Coate JE. 2014. The legacy of diploid progenitors in allopolyploid gene expression patterns. *Philosophical Transactions of the Royal Society, B: Biological Sciences* **369**: 20130354.

Buggs RJA, Zhang L, Miles N, Tate JA, Gao L, Wei W, Schnable PS, Barbazuk WB, Soltis PS, Soltis DE. 2011. Transcriptomic shock generates evolutionary novelty in a newly formed, natural allopolyploid plant. *Current Biology* **21**: 551–556.

Burton WG, Grabowy CT, Sager R. 1979. Role of methylation in the modification and restriction of chloroplast DNA in Chlamydomonas. *Proceedings of the National Academy of Sciences, USA* **76**: 1390–1394.

Bushnell B. 2014. *BBMap: a fast, accurate, splice-aware aligner*. Berkeley, CA, USA: Lawrence Berkeley National Lab (LBNL).

Čertnerová D, Galbraith DW. 2021. Best practices in the flow cytometry of microalgae. *Cytometry, Part A* **99**: 359–364.

Chagué V, Just J, Mestiri I, Balzergue S, Tanguy A-M, Huneau C, Huteau V, Belcram H, Coriton O, Jahier J *et al.* 2010. Genome-wide gene expression changes in genetically stable synthetic and natural wheat allohexaploids. *New Phytologist* **187**: 1181–1194.

Chelaifa H, Chagué V, Chalabi S, Mestiri I, Arnaud D, Deffains D, Lu Y, Belcram H, Huteau V, Chiquet J *et al.* 2013. Prevalence of gene expression additivity in genetically stable wheat allohexaploids. *New Phytologist* **197**: 730–736.

Chelaifa H, Monnier A, Ainouche M. 2010. Transcriptomic changes following recent natural hybridization and allopolyploidy in the salt marsh species Spartina × townsendii and Spartina anglica (Poaceae). *New Phytologist* **186**: 161–174.

Chester M, Gallagher JP, Symonds VV, Silva AVC d, Mavrodiev EV, Leitch AR, Soltis PS, Soltis DE. 2012. Extensive chromosomal variation in a recently formed natural allopolyploid species, *Tragopogon miscellus* (Asteraceae). *Proceedings of the National Academy of Sciences, USA* **109**: 1176–1181.

Coate JE, Doyle JJ. 2013. Genomics and transcriptomics of photosynthesis in polyploids. In: *Polyploid and hybrid genomics*. New York, NY, USA: John Wiley & Sons, Ltd, 153–169.

Coate JE, Luciano AK, Seralathan V, Minchew KJ, Owens TG, Doyle JJ. 2012. Anatomical, biochemical, and photosynthetic responses to recent allopolyploidy in Glycine dolichocarpa (Fabaceae). *American Journal of Botany* **99**: 55–67.

Coate JE, Schreyer WM, Kum D, Doyle JJ. 2020. Robust cytonuclear coordination of transcription in nascent *Arabidopsis thaliana* autopolyploids. *Genes* **11**: 134.

Comai L. 2005. The advantages and disadvantages of being polyploid. *Nature Reviews Genetics* **6**: 836–846.

Combes M-C, Hueber Y, Dereeper A, Rialle S, Herrera J-C, Lashermes P. 2015. Regulatory divergence between parental alleles determines gene expression patterns in hybrids. *Genome Biology and Evolution* **7**: 1110–1121.

Craig RJ, Gallaher SD, Shu S, Salomé PA, Jenkins JW, Blaby-Haas CE, Purvine SO, O'Donnell S, Barry K, Grimwood J *et al.* 2023. The Chlamydomonas Genome Project, v.6: reference assemblies for mating-type plus and minus strains reveal extensive structural mutation in the laboratory. *Plant Cell* **35**: 644–672.

De Smet R, Van de Peer Y. 2012. Redundancy and rewiring of genetic networks following genome-wide duplication events. *Current Opinion in Plant Biology* **15**: 168–176.

Doyle JJ, Coate JE. 2019. Polyploidy, the nucleotype, and novelty: the impact of genome doubling on the biology of the cell. *International Journal of Plant Sciences* **180**: 1–52.

Doyle JJ, Flagel LE, Paterson AH, Rapp RA, Soltis DE, Soltis PS, Wendel JF. 2008. Evolutionary genetics of genome merger and doubling in plants. *Annual Review of Genetics* **42**: 443–461.

Dpooležel J, Binarová P, Lcretti S. 1989. Analysis of nuclear DNA content in plant cells by flow cytometry. *Biologia Plantarum* **31**: 113–120.

Ebersold WT. 1967. *Chlamydomonas reinhardi*: heterozygous diploid strains. *Science* **157**: 447–449.

Edger PP, Smith R, McKain MR, Cooley AM, Vallejo-Marin M, Yuan Y, Bewick AJ, Ji L, Platts AE, Bowman MJ *et al.* 2017. Subgenome dominance in an interspecific hybrid, synthetic allopolyploid, and a 140-year-old naturally established neo-allopolyploid monkeyflower. *Plant Cell* **29**: 2150–2167.

Fawcett JA, Maere S, Van de Peer Y. 2009. Plants with double genomes might have had a better chance to survive the Cretaceous–Tertiary extinction event. *Proceedings of the National Academy of Sciences, USA* **106**: 5737–5742.

Fernandes Gyorfy M, Miller ER, Conover JL, Grover CE, Wendel JF, Sloan DB, Sharbrough J. 2021. Nuclear–cytoplasmic balance: whole genome duplications induce elevated organellar genome copy number. *The Plant Journal* **108**: 219–230.

Flagel LE, Wendel JF. 2010. Evolutionary rate variation, genomic dominance and duplicate gene expression evolution during allotetraploid cotton speciation. *New Phytologist* **186**: 184–193.

Forsythe ES, Grover CE, Miller ER, Conover JL, Arick MA, Chavarro MCF, Leal-Bertioli SCM, Peterson DG, Sharbrough J, Wendel JF *et al.* 2022. Organellar transcripts dominate the cellular mRNA pool across plants of varying ploidy levels. *Proceedings of the National Academy of Sciences, USA* **119**: e2204187119.

Fox DT, Soltis DE, Soltis PS, Ashman T-L, Van de Peer Y. 2020. Polyploidy: a biological force from cells to ecosystems. *Trends in Cell Biology* **30**: 688–694.

Ganem NJ, Storchova Z, Pellman D. 2007. Tetraploidy, aneuploidy and cancer. *Current Opinion in Genetics & Development* **17**: 157–162.

Gerstein AC, Chun H-JE, Grant A, Otto SP. 2006. Genomic convergence toward diploidy in *Saccharomyces cerevisiae*. *PLoS Genetics* **2**: e145.

Gerstein AC, Fu MS, Mukaremera L, Li Z, Ormerod KL, Fraser JA, Berman J, Nielsen K. 2015. Polyploid titan cells produce haploid and aneuploid progeny to promote stress adaptation. *MBio* **6**: 1340.

Gillham NW. 1969. Uniparental inheritance in *Chlamydomonas reinhardi*. *The American Naturalist* **103**: 355–388.

Glombik M, Copetti D, Bartos J, Stoces S, Zwierzykowski Z, Ruttink T, Wendel JF, Duchoslav M, Dolezel J, Studer B *et al.* 2021. Reciprocal allopolyploid grasses (Festuca × Lolium) display stable patterns of genome dominance. *The Plant Journal* **107**: 1166–1182.

Gou X, Bian Y, Zhang A, Zhang H, Wang B, Lv R, Li J, Zhu B, Gong L, Liu B. 2018. Transgenerationally precipitated meiotic chromosome instability fuels rapid karyotypic evolution and phenotypic diversity in an artificially constructed allotetraploid wheat (AADD). *Molecular Biology and Evolution* **35**: 1078–1091.

Grover CE, Forsythe ES, Sharbrough J, Miller ER, Conover JL, DeTar RA, Chavarro C, Arick MA II, Peterson DG, Leal-Bertioli SCM *et al.* 2022. Variation in cytonuclear expression accommodation among allopolyploid plants. *Genetics* **222**: 118.

Grover CE, Gallagher JP, Szadkowski EP, Yoo MJ, Flagel LE, Wendel JF. 2012. Homoeolog expression bias and expression level dominance in allopolyploids. *New Phytologist* **196**: 966–971.

Harris EH. 2001. Chlamydomonas as a model organism. *Annual Review of Plant Physiology and Plant Molecular Biology* **52**: 363–406.

Hegarty MJ, Barker GL, Wilson ID, Abbott RJ, Edwards KJ, Hiscock SJ. 2006. Transcriptome shock after interspecific hybridization in senecio is ameliorated by genome duplication. *Current Biology* **16**: 1652–1659.

Hegarty MJ, Hiscock SJ. 2009. The complex nature of allopolyploid plant genomes. *Heredity* **103**: 100–101.

Heifetz PB, Förster B, Osmond CB, Giles LJ, Boynton JE. 2000. Effects of acetate on facultative autotrophy in *Chlamydomonas reinhardtii* assessed by photosynthetic measurements and stable isotope analyses. *Plant Physiology* **122**: 1439–1446.

Hessen DO, Jeyasingh PD, Neiman M, Weider LJ. 2010. Genome streamlining and the elemental costs of growth. *Trends in Ecology & Evolution* **25**: 75–80.

Hickman MA, Paulson C, Dudley A, Berman J. 2015. Parasexual ploidy reduction drives population heterogeneity through random and transient aneuploidy in *Candida albicans*. *Genetics* **200**: 781–794.

Hlavová M, Vítová M, Bišová K. 2016. Synchronization of green algae by light and dark regimes for cell cycle and cell division studies. In: Caillaud M-C, ed. *Methods in molecular biology. Plant cell division: methods and protocols*. New York, NY, USA: Springer, 3–16.

Ilut DC, Coate JE, Luciano AK, Owens TG, May GD, Farmer A, Doyle JJ. 2012. A comparative transcriptomic study of an allotetraploid and its diploid progenitors illustrates the unique advantages and challenges of RNA-seq in plant species. *American Journal of Botany* **99**: 383–396.

Jeong H, Mason SP, Barabási A-L, Oltvai ZN. 2001. Lethality and centrality in protein networks. *Nature* **411**: 41–42.

Jia Z, Gao P, Yin F, Quilichini TD, Sheng H, Song J, Yang H, Gao J, Chen T, Yang B *et al.* 2022. Asymmetric gene expression in grain development of reciprocal crosses between tetraploid and hexaploid wheats. *Communications Biology* **5**: 1–15.

Kim D, Paggi JM, Park C, Bennett C, Salzberg SL. 2019. Graph-based genome alignment and genotyping with HISAT2 and HISAT-genotype. *Nature Biotechnology* **37**: 907–915.

Kuroiwa T, Kawano S, Nishibayashi S, Sato C. 1982. Epifluorescent microscopic evidence for maternal inheritance of chloroplast DNA. *Nature* **298**: 481–483.

Kwak M, Park W-K, Shin S-E, Koh H-G, Lee B, Jeong B, Chang YK. 2017. Improvement of biomass and lipid yield under stress conditions by using diploid strains of *Chlamydomonas reinhardtii*. *Algal Research* **26**: 180–189.

Leebens-Mack JH, Barker MS, Carpenter EJ, Deyholos MK, Gitzendanner MA, Graham SW, Grosse I, Li Z, Melkonian M, Mirarab S *et al.* 2019. One thousand plant transcriptomes and the phylogenomics of green plants. *Nature* **574**: 679–685.

Li A, Liu D, Wu J, Zhao X, Hao M, Geng S, Yan J, Jiang X, Zhang L, Wu J *et al.* 2014. mRNA and Small RNA transcriptomes reveal insights into dynamic homoeolog regulation of allopolyploid heterosis in nascent hexaploid wheat. *Plant Cell* **26**: 1878–1900.

Li M, Wang R, Wu X, Wang J. 2020. Homoeolog expression bias and expression level dominance (ELD) in four tissues of natural allotetraploid Brassica napus. *BMC Genomics* **21**: 330.

Li W, Liu J, Tan H, Luo L, Cui J, Hu J, Wang S, Liu Q, Hu F, Tang C *et al.* 2018. Asymmetric expression patterns reveal a strong maternal effect and dosage compensation in polyploid hybrid fish. *BMC Genomics* **19**: 517.

Li Z, McKibben MTW, Finch GS, Blischak PD, Sutherland BL, Barker MS. 2021. Patterns and processes of diploidization in land plants. *Annual Review of Plant Biology* **72**: 387–410.

Loppes R. 1969. A new class of arginine-requiring mutants in *Chlamydomonas reinhardi*. *Molecular and General Genetics MGG* **104**: 172–177.

Love MI, Huber W, Anders S. 2014. Moderated estimation of fold change and dispersion for RNA-seq data with DESeq2. *Genome Biology* **15**: 550.

Lu Y-J, Swamy KBS, Leu J-Y. 2016. Experimental evolution reveals interplay between Sch9 and polyploid stability in yeast. *PLoS Genetics* **12**: e1006409.

Lv R, Wang C, Wang R, Wang X, Zhao J, Wang B, Aslam T, Han F, Liu B. 2022. Chromosomal instability and phenotypic variation in a specific lineage derived from a synthetic allotetraploid wheat. *Frontiers in Plant Science* **13**: 1218.

Ma X-F, Gustafson JP. 2005. Genome evolution of allopolyploids: a process of cytological and genetic diploidization. *Cytogenetic and Genome Research* **109**: 236–249.

Mable BK. 2013. Polyploids and hybrids in changing environments: winners or losers in the struggle for adaptation? *Heredity* **110**: 95–96.

Malerba ME, Ghedini G, Marshall DJ. 2020. Genome size affects fitness in the eukaryotic alga *Dunaliella tertiolecta*. *Current Biology* **30**: 3450–3456.e3.

Malerba ME, Palacios MM, Palacios Delgado YM, Beardall J, Marshall DJ. 2018. Cell size, photosynthesis and the package effect: an artificial selection approach. *New Phytologist* **219**: 449–461.

Marguerat S, Bähler J. 2012. Coordinating genome expression with cell size. *Trends in Genetics* **28**: 560–565.

McClintock B. 1984. The significance of responses of the genome to challenge. *Science* **226**: 792–801.

Mestiri I, Chagué V, Tanguy A-M, Huneau C, Huteau V, Belcram H, Coriton O, Chalhoub B, Jahier J. 2010. Newly synthesized wheat allohexaploids display progenitor-dependent meiotic stability and aneuploidy but structural genomic additivity. *New Phytologist* **186**: 86–101.

Moll P, Ante M, Seitz A, Reda T. 2014. QuantSeq 3′ mRNA sequencing for RNA quantification. *Nature Methods* **11**: i–iii.

Nakamura S. 2010. Paternal inheritance of mitochondria in Chlamydomonas. *Journal of Plant Research* **123**: 163–170.

Nieto Feliner G, Casacuberta J, Wendel JF. 2020. Genomics of evolutionary novelty in hybrids and polyploids. *Frontiers in Genetics* **11**: 2204.

Oberprieler C, Talianova M, Griesenbeck J. 2019. Effects of polyploidy on the coordination of gene expression between organellar and nuclear genomes in Leucanthemum Mill. (Compositae, Anthemideae). *Ecology and Evolution* **9**: 9100–9110.

Osborn TC, Chris Pires J, Birchler JA, Auger DL, Jeffery Chen Z, Lee H-S, Comai L, Madlung A, Doerge RW, Colot V *et al.* 2003. Understanding mechanisms of novel gene expression in polyploids. *Trends in Genetics* **19**: 141–147.

Otto SP. 2003. In polyploids, one plus one does not equal two. *Trends in Ecology & Evolution* **18**: 431–433.

Otto SP. 2007. The evolutionary consequences of polyploidy. *Cell* **131**: 452–462.

Otto SP, Whitton J. 2000. Polyploid incidence and evolution. *Annual Review of Genetics* **34**: 401–437.

Parisod C, Holderegger R, Brochmann C. 2010. Evolutionary consequences of autopolyploidy: research review. *New Phytologist* **186**: 5–17.

Qi B, Huang W, Zhu B, Zhong X, Guo J, Zhao N, Xu C, Zhang H, Pang J, Han F *et al.* 2012. Global transgenerational gene expression dynamics in two newly synthesized allohexaploid wheat (*Triticum aestivum*) lines. *BMC Biology* **10**: 3.

Raina SN, Parida A, Koul KK, Salimath SS, Bisht MS, Raja V, Khoshoo TN. 1994. Associated chromosomal DNA changes in polyploids. *Genome* **37**: 560–564.

Rapp RA, Udall JA, Wendel JF. 2009. Genomic expression dominance in allopolyploids. *BMC Biology* 7: 18.

Ratcliff WC, Herron MD, Howell K, Pentz JT, Rosenzweig F, Travisano M. 2013. Experimental evolution of an alternating uni- and multicellular life cycle in *Chlamydomonas reinhardtii*. *Nature Communications* **4**: 2742.

Ritchie SC, Watts S, Fearnley LG, Holt KE, Abraham G, Inouye M. 2016. A scalable permutation approach reveals replication and preservation patterns of network modules in large datasets. *Cell Systems* **3**: 71–82.

Salomé PA, Merchant SS. 2019. A series of fortunate events: introducing chlamydomonas as a reference organism. *Plant Cell* **31**: 1682–1707.

Sasso S, Stibor H, Mittag M, Grossman AR. 2018. From molecular manipulation of domesticated *Chlamydomonas reinhardtii* to survival in nature. *eLife* **7**: e39233.

Scranton MA, Ostrand JT, Fields FJ, Mayfield SP. 2015. Chlamydomonas as a model for biofuels and bio-products production. *The Plant Journal* **82**: 523–531.

Seervai RNH, Jones SK, Hirakawa MP, Porman AM, Bennett RJ. 2013. Parasexuality and ploidy change in *Candida tropicalis*. *Eukaryotic Cell* **12**: 1629–1640.

Shahbazi M, Majka J, Kubíková D, Zwierzykowski Z, Glombik M, Wendel JF, Sharbrough J, Hartmann S, Szecówka M, Doležel J *et al.* 2024. Cytonuclear interplay in auto- and allopolyploids: a multifaceted perspective from the Festuca-Lolium complex. *The Plant Journal* **118**: 1102–1118.

Sharbrough J, Conover JL, Tate JA, Wendel JF, Sloan DB. 2017. Cytonuclear responses to genome doubling. *American Journal of Botany* **104**: 1277–1280.

Shimizu KK. 2022. Robustness and the generalist niche of polyploid species: genome shock or gradual evolution? *Current Opinion in Plant Biology* **69**: 102292.

Shimizu-Inatsugi R, Terada A, Hirose K, Kudoh H, Sese J, Shimizu KK. 2017. Plant adaptive radiation mediated by polyploid plasticity in transcriptomes. *Molecular Ecology* **26**: 193–207.

Sloan DB, Conover JL, Grover CE, Wendel JF, Sharbrough J. 2024. Polyploid plants take cytonuclear perturbations in stride. *Plant Cell* **36**: 829–839.

Smith T, Heger A, Sudbery I. 2017. UMI-tools: modeling sequencing errors in unique molecular identifiers to improve quantification accuracy. *Genome Research* **27**: 491–499.

Soltis DE, Albert VA, Leebens-Mack J, Bell CD, Paterson AH, Zheng C, Sankoff D, Pamphilis CW, Wall PK, Soltis PS. 2009. Polyploidy and angiosperm diversification. *American Journal of Botany* **96**: 336–348.

Soltis DE, Buggs RJA, Doyle JJ, Soltis PS. 2010. What we still don't know about polyploidy. *Taxon* **59**: 1387–1403.

Soltis DE, Misra BB, Shan S, Chen S, Soltis PS. 2016. Polyploidy and the proteome. *Biochimica et Biophysica Acta (BBA) – Proteins and Proteomics* **1864**: 896–907.

Song H-S, McClure RS, Bernstein HC, Overall CC, Hill EA, Beliaev AS. 2015. Integrated *in silico* analyses of regulatory and metabolic networks of *Synechococcus* sp. PCC 7002 reveal relationships between gene centrality and essentiality. *Lifestyles* **5**: 1127–1140.

Song K, Lu P, Tang K, Osborn TC. 1995. Rapid genome change in synthetic polyploids of Brassica and its implications for polyploid evolution. *Proceedings of the National Academy of Sciences, USA* **92**: 7719–7723.

Song MJ, Potter BI, Doyle JJ, Coate JE. 2020. Gene balance predicts transcriptional responses immediately following ploidy change in *Arabidopsis thaliana*. *Plant Cell* **32**: 1434–1448.

Spoelhof JP, Soltis PS, Soltis DE. 2017. Pure polyploidy: closing the gaps in autopolyploid research: pure polyploidy. *Journal of Systematics and Evolution* **55**: 340–352.

Stebbins GL. 1947. Types of polyploids: their classification and significance. In: Demerec M, ed. *Advances in genetics*. New York, NY, USA: Academic Press, 403–429.

Storchova Z. 2014. Ploidy changes and genome stability in yeast. *Yeast* **31**: 421–430.

Storchova Z, Pellman D. 2004. From polyploidy to aneuploidy, genome instability and cancer. *Nature Reviews Molecular Cell Biology* **5**: 45–54.

Tate JA, Symonds VV, Doust AN, Buggs RJA, Mavrodiev E, Majure LC, Soltis PS, Soltis DE. 2009. Synthetic polyploids of *Tragopogon miscellus* and *T. mirus* (Asteraceae): 60 years after Ownbey's discovery. *American Journal of Botany* **96**: 979–988.

Thompson SL, Bakhoum SF, Compton DA. 2010. Mechanisms of chromosomal instability. *Current Biology* **20**: R285–R295.

Thompson SL, Compton DA. 2008. Examining the link between chromosomal instability and aneuploidy in human cells. *Journal of Cell Biology* **180**: 665–672.

Tsukaya H. 2013. Does ploidy level directly control cell size? Counterevidence from Arabidopsis genetics. *PLoS ONE* **8**: e83729.

Van de Peer Y, Ashman T-L, Soltis PS, Soltis DE. 2021. Polyploidy: an evolutionary and ecological force in stressful times. *Plant Cell* **33**: 11–26.

Van de Peer Y, Mizrachi E, Marchal K. 2017. The evolutionary significance of polyploidy. *Nature Reviews Genetics* **18**: 411–424.

Vanneste K, Baele G, Maere S, Van de Peer Y. 2014. Analysis of 41 plant genomes supports a wave of successful genome duplications in association with the Cretaceous–Paleogene boundary. *Genome Research* **24**: 1334–1347.

Vyas P, Bisht MS, Miyazawa S-I, Yano S, Noguchi K, Terashima I, Funayama-Noguchi S. 2007. Effects of polyploidy on photosynthetic properties and anatomy in leaves of Phlox drummondii. *Functional Plant Biology* **34**: 673–682.

Wang J, Tian L, Lee H-S, Chen ZJ. 2006. Nonadditive regulation of FRI and FLC loci mediates flowering-time variation in Arabidopsis allopolyploids. *Genetics* **173**: 965–974.

Wang X, Morton JA, Pellicer J, Leitch IJ, Leitch AR. 2021. Genome downsizing after polyploidy: mechanisms, rates and selection pressures. *The Plant Journal* **107**: 1003–1015.

Warner DA, Edwards GE. 1993. Effects of polyploidy on photosynthesis. *Photosynthesis Research* **35**: 135–147.

Wei Y, Li G, Zhang S, Zhang S, Zhang H, Sun R, Zhang R, Li F. 2021. Analysis of transcriptional changes in different Brassica *napus* synthetic allopolyploids. *Genes* **12**: 82.

Wendel JF, Lisch D, Hu G, Mason AS. 2018. The long and short of doubling down: polyploidy, epigenetics, and the temporal dynamics of genome fractionation. *Current Opinion in Genetics & Development* **49**: 1–7.

Whiteway MS, Lee RW. 1977. Chloroplast DNA content increases with nuclear ploidy in Chlamydomonas. *MGG Molecular & General Genetics* **157**: 11–15.

Wu C-Y, Rolfe PA, Gifford DK, Fink GR. 2010. Control of transcription by cell size. *PLoS Biology* **8**: e1000523.

Wu J, Lin L, Xu M, Chen P, Liu D, Sun Q, Ran L, Wang Y. 2018. Homoeolog expression bias and expression level dominance in resynthesized allopolyploid *Brassica napus*. *BMC Genomics* **19**: 586.

Xiong Z, Gaeta RT, Pires JC. 2011. Homoeologous shuffling and chromosome compensation maintain genome balance in resynthesized allopolyploid *Brassica napus*. *Proceedings of the National Academy of Sciences, USA* **108**: 7908–7913.

Yoo M-J, Liu X, Pires JC, Soltis PS, Soltis DE. 2014. Nonadditive gene expression in polyploids. *Annual Review of Genetics* **48**: 485–517.

Yoo M-J, Szadkowski E, Wendel JF. 2013. Homoeolog expression bias and expression level dominance in allopolyploid cotton. *Heredity* **110**: 171–180.

Yu H, Greenbaum D, Lu HX, Zhu X, Gerstein M. 2004. Genomic analysis of essentiality within protein networks. *Trends in Genetics* **20**: 227–231.

Zhang D, Pan Q, Tan C, Zhu B, Ge X, Shao Y, Li Z. 2016. Genome-wide gene expressions respond differently to A-subgenome origins in brassica napus synthetic hybrids and natural allotetraploid. *Frontiers in Plant Science* **7**: 2587.

Zhang H, Bian Y, Gou X, Zhu B, Xu C, Qi B, Li N, Rustgi S, Zhou H, Han F *et al.* 2013. Persistent whole-chromosome aneuploidy is generally associated with nascent allohexaploid wheat. *Proceedings of the National Academy of Sciences, USA* **110**: 3447–3452.

Zhang M, Tang Y-W, Qi J, Liu X-K, Yan D-F, Zhong N-S, Tao N-Q, Gao J-Y, Wang Y-G, Song Z-P *et al.* 2019. Effects of parental genetic divergence on gene expression patterns in interspecific hybrids of Camellia. *BMC Genomics* **20**: 828.

Zhou P, Hirsch CN, Briggs SP, Springer NM. 2019. Dynamic patterns of gene expression additivity and regulatory variation throughout maize development. *Molecular Plant* **12**: 410–425.

Zotenko E, Mestre J, O'Leary DP, Przytycka TM. 2008. Why do hubs in the yeast protein interaction network tend to be essential: reexamining the connection between the network topology and essentiality. *PLoS Computational Biology* **4**: e1000140.

Supporting Information

Additional Supporting Information may be found online in the Supporting Information section at the end of the article.

Fig. S1 Growth curves of the different experimental strains.

Fig. S2 Mean maximum growth rate of parental strains, ancestral triploid, and triploid lines pooled at generation time points (G225 and G425).

Fig. S3 Comparative flow cytometric analysis of propidium iodide-stained nuclei for genome size estimation.

Fig. S4 Conservation of expression patterns across three experimental evolution time points (G0, G225, and G425) in the triploid progeny lines.

Fig. S5 Summary statistics of coexpression modules for the network with all samples.

Table S1 Overrepresented KEGG pathways among persistent downregulated genes in the triploid.

Table S2 Overrepresented KEGG pathways among genes showing persistent expression level dominance toward the haploid parent (ELD1).

Table S3 Overrepresented Gene Ontology terms in Category II genes.

Table S4 Overrepresented Gene Ontology terms in Category XI genes.

Table S5 Overview of genes in the lightsteelblue module.

Please note: Wiley is not responsible for the content or functionality of any Supporting Information supplied by the authors. Any queries (other than missing material) should be directed to the *New Phytologist* Central Office.